ORIGINAL ARTICLE

# Evaluation of a Novel Time-Efficient Protocol for Gadobenate Dimeglumine (Gd-BOPTA)-Enhanced Liver Magnetic Resonance Imaging

*Günther Schneider, MD,\* Katrin Altmeyer, MD,\* Miles A. Kirchin, PhD,† Roland Seidel, MD,\* Luigi Grazioli, MD,‡ Giovanni Morana, MD,§ and Sanjay Saini, MD¶*

**Objective:** We sought to evaluate gadobenate dimeglumine for the detection and characterization of focal liver lesions in the unenhanced and already pre-enhanced liver.

**Materials and Methods:** Sixty patients were evaluated prospectively. Unenhanced T1-weighted gradient echo (T1wGRE) and T2-weighted turbo spin echo (T2wTSE) images were acquired followed by contrast-enhanced T1wGRE images during the dynamic, equilibrium, and delayed phases after the bolus injection of 0.05 mmol/kg gadobenate dimeglumine. An identical series of dynamic images was then acquired after the delayed scan following a second 0.05 mmol/kg bolus of gadobenate dimeglumine. Images were evaluated randomly in 2 sessions by 3 independent blinded readers. Evaluated images in the first session comprised the unenhanced images, the first or second set of dynamic images, and the delayed images. The second session included the unenhanced images, the dynamic images not yet evaluated in the first session, and the delayed images. The 2 reading sessions were compared for lesion characterization and diagnosis, and kappa ($\kappa$) values for interobserver agreement were determined. Quantitative evaluation of lesion contrast enhancement was also performed.

**Results:** The enhancement behavior in the second dynamic series was similar to that in the first series, although pre-enhancement of the normal liver resulted in reduced lesion-liver contrast-to-noise ratios and the visualization of some lesions only on arterial phase images. Typical imaging features for the lesions included in the study were visualized clearly in both series. Strong agreement ($\kappa$ = 0.56–0.89; all evaluations) between the 2 images sets was noted by all readers for differentiation of benign from malignant lesions and for definition of specific diagnosis, and between readers for diagnoses established based on images acquired in the unenhanced and pre-enhanced liver.

**Conclusion:** Dynamic imaging in the hepatobiliary phase gives similar information as dynamic imaging of the unenhanced liver. This might prove advantageous for screening protocols involving same session imaging of primary extrahepatic tumors and liver.

**Key Words:** gadobenate dimeglumine, liver imaging, MR protocol, MR imaging

(*Invest Radiol* 2007;42: 105–115)

G adobenate dimeglumine (Gd-BOPTA, MultiHance; Bracco Imaging SpA, Milan, Italy) is a gadolinium-based MR contrast agent with 2 unique features compared with conventional gadolinium contrast agents. First, it possesses high r1- and r2-relaxivity in blood at all magnetic field strengths because of weak, transient interactions of the Gd-BOPTA contrast-effective moiety with serum albumin.[1–3] Values for r1-relaxivity of 10.9, 7.9, and 5.9 $L \cdot mmol^{-1}s^{-1}$ have recently been reported for gadobenate dimeglumine in human blood plasma (37°C) at magnetic field strengths of 0.2, 1.5, and 3 T, respectively, compared with 5.7, 3.9, and 3.9 $L \cdot mmol^{-1}s^{-1}$, respectively, for gadopentetate dimeglumine under the same conditions.[1] The increased r1- and r2-relaxivity of gadobenate dimeglumine leads to considerably greater contrast enhancement for magnetic resonance imaging (MRI) applications in general[4–9] and liver imaging in particular.[10,11] Second, gadobenate dimeglumine has a dual route of elimination with 3–5% of the injected dose taken up by functioning hepatocytes and eliminated in the bile.[12,13] Although the fraction eliminated through the hepatobiliary pathway does not affect the overall pharmacokinetic profile compared with other gadolinium agents,[12] or the ability to perform dynamic imaging of the liver after bolus injection,[11,14–17] the 3–5% taken up leads to a marked and prolonged enhancement of healthy liver parenchyma[18] against which primary malignant tumors and secondary metastases generally appear hypointense on images acquired at 1–3 hours after injection as a result of the absence of functioning hepatocytes within these lesions. Several studies have demonstrated improved liver lesion detection on delayed MRI with gadobenate dimeglumine.[12,14–17,19,20] The value of

noses established based on images acquired in the unenhanced and pre-enhanced liver.

delayed MRI with gadobenate dimeglumine for improved liver lesion characterization has also been demonstrated, particularly for the characterization of atypical focal nodular hyperplasia (FNH)[21] and for the accurate differential diagnosis of FNH from hepatic adenoma.[22]

However, although the possibility to perform delayed hepatobiliary phase imaging has proven advantageous for many clinical questions, the imaging protocol routinely used at most institutions requires an interval of 1–3 hours between the initial dynamic examination and the delayed hepatobiliary examination. With this in mind, the present study was conducted in patients with focal liver lesions to determine the feasibility of a more time-efficient imaging protocol in which the delayed phase examination is performed before the dynamic phase examination. The principal objective was to demonstrate equivalence between the liver lesion enhancement patterns observed on conventional dynamic imaging using a standard imaging protocol, and those observed on contrast-enhanced dynamic imaging in a previously contrast-enhanced liver. Favorable results might positively impact the clinical application of gadolinium contrast agents with hepatobiliary properties, permitting initial screening for liver metastases and, if necessary, accurate same-session dynamic characterization of equivocal incidental lesions.

## MATERIALS AND METHODS

### Subjects

Sixty consecutive patients (28 men, 32 women; mean age 52 ± 14 years; range 27–75 years) with one or more focal liver lesions detected at sonography and/or computed tomography and subsequently referred for contrast-enhanced MRI were included in the study. All patients were examined as part of clinical routine. On the basis of all imaging findings, 30 patients were diagnosed with primary (n = 9) or secondary (n = 21) malignant lesions and 30 patients with benign lesions.

### Patients With Malignant Lesions

The 9 patients with primary malignant lesions comprised 6 patients with hepatocellular carcinoma (HCC; 2 patients with a single lesion only, 1 patient with a single HCC and a pseudolesion [transitory hepatic attenuation difference], 1 patient with 2 atypical HCC nodules and 2 cysts, and 2 patients each with more than 10 HCC lesions, one of whom had alcohol-induced cirrhosis), 2 patients with fibrolamellar carcinoma (both of whom had one or more surrounding daughter nodules), and 1 patient with cholangiocellular carcinoma. The 21 patients with liver metastases comprised 4 patients with primary breast cancer (1 with a single metastatic lesion, another with 2 lesions, and the remaining 2 patients with more than 10 lesions each), 4 patients with primary colorectal carcinoma (1 patient with 6 metastatic lesions, 1 patient with 3 lesions, and 2 patients with 2 lesions each), 2 patients with primary leiomyosarcoma (1 patient with a single metastatic lesion and the other with more than 30 lesions), 1 patient with 3 metastatic lesions from primary gastric cancer and 2 cysts, 1 patient with 7 metastatic lesions from primary esophageal 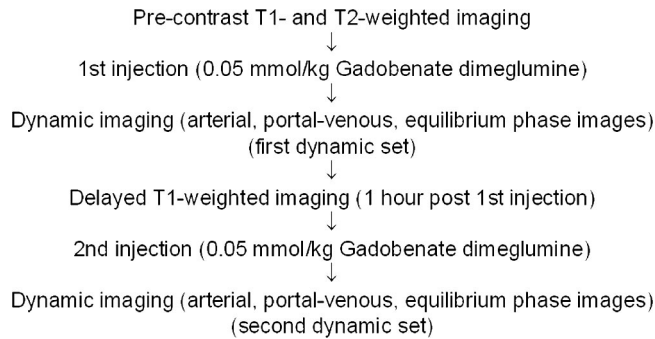cancer, 1 patient with more than 10 metastatic lesions from primary renal cell carcinoma, 1 patient with more than 40 metastatic lesions from primary lung adenocarcinoma, 1 patient with a single metastatic lesion from primary adenocarcinoma of the appendix, 1 patient with more than 20 metastatic lesions from an unknown primary adenocarcinoma, 1 patient with a single intrahepatic metastasis from previously resected cholangiocarcinoma, and 1 patient with a single hypervascular metastasis from an unknown primary tumor and one cyst. The remaining 3 patients with metastases also were shown on on-site final diagnosis to have additional benign hemangiomas. Two of these patients had primary melanoma (1 with more than 10 metastatic lesions and 2 hemangiomas and the other with a single metastatic lesion, 2 hemangiomas and 5 cysts) whereas the third patient, who suffered from a primary carcinoid, had 10 metastatic lesions and 2 hemangiomas.

### Patients With Benign Lesions

The most frequent lesions among the 30 subjects with benign liver lesions were hemangioma and focal nodular hyperplasia (FNH). Overall, 11 subjects were diagnosed with hemangioma alone (7 patients with a solitary hemangioma, 1 of whom also had 3 cysts and another 2 cysts; 3 patients with 2 hemangiomas, 1 with both a capillary and a cavernous hemangioma and another with an additional cyst; and 1 patient with 3 hemangiomas and a cyst). A further 6 subjects were diagnosed with FNH alone (2 subjects with solitary typical FNH, 1 of whom also had an additional cyst, 2 subjects with solitary atypical FNH, and 2 subjects with 3 FNH each). Two subjects were diagnosed with both hemangioma and FNH (one subject with 2 hemangiomas and 1 atypical FNH and the other subject with 1 hemangioma and 2 FNH). One further subject with an FNH nodule was diagnosed principally as having adenomatosis (7 adenomas detected on on-site final diagnosis). The remaining patients with diagnosed benign lesions comprised 1 patient with a solitary adenoma, 3 subjects with regenerative nodules (2 subjects with a single lesion each and one subject with 2 lesions), 1 subject with a solitary nodule of regenerative hyperplasia, 1 subject with post-traumatic subcapsular hematoma, 1 subject with postsurgical bilioma and 14 cysts, 1 subject with a single inflammatory pseudotumor, 1 subject with a single echinococcal cyst, and 1 subject with multiple abscess formations.

### MRI Protocol

All patients were studied on a 1.5 T MR unit (Magnetom Vision, Siemens Medical Systems, Erlangen, Germany) at a single center using a body-array coil. MRI in all patients was performed using T2-weighted turbo spin echo (T2wTSE) sequences, T2-weighted HASTE (T2w-HASTE) sequences, and T1-weighted gradient echo FLASH-2D (T1wGRE) sequences according to the scheme shown in Figure 1. T2-weighted imaging was performed with both TSE and HASTE sequences to obtain satisfactory T2-weighted images in all patients (ie, to avoid limitations associated with comparatively high motion sensitivity in the case of T2wTSE sequences, eg, caused by bowel movement in bowel loops adjacent to the liver and reduced lesion-to-liver contrast in the

Pre-contrast T1- and T2-weighted imaging
↓
1st injection (0.05 mmol/kg Gadobenate dimeglumine)
↓
Dynamic imaging (arterial, portal-venous, equilibrium phase images)
(first dynamic set)
↓
Delayed T1-weighted imaging (1 hour post 1st injection)
↓
2nd injection (0.05 mmol/kg Gadobenate dimeglumine)
↓
Dynamic imaging (arterial, portal-venous, equilibrium phase images)
(second dynamic set)

**FIGURE 1.** Contrast administration and image acquisition scheme.

case of T2w-HASTE sequences, eg, in case of metastases of colorectal tumors). Images were acquired before the administration of gadobenate dimeglumine (unenhanced T2w and T1wGRE images), during the dynamic phase of contrast enhancement after the intravenous bolus administration of 0.05 mmol/kg bodyweight gadobenate dimeglumine (T1wGRE images only, acquired at 20 to 25s [arterial phase], 55 to 60s [portal-venous phase], and 3 to 5 minutes [equilibrium phase] postinjection), and in a delayed hepatobiliary phase after the administration of gadobenate dimeglumine (T1wGRE images only, acquired at 1 hour after injection). A second bolus injection of 0.05 mmol/kg bodyweight gadobenate dimeglumine (same parameters as the first injection) followed by acquisition of a second, identical series of dynamic phase images was then performed immediately after the delayed (hepatobiliary) scan (Fig. 1). Gadobenate dimeglumine was administered to all patients by means of a power injector (Injektron MRT, MEDTRON, Germany) via an antecubital vein of the right arm at a rate of 2.5 mL/s. All injections were followed by a 20-mL saline flush at the same rate.

Precontrast T2wTSE images were acquired with TR = 3200 milliseconds, TE = 138 milliseconds. A total of 22 slices were acquired in 2 breath-holds (11 slices/breath-hold) with an overall imaging time of 17 seconds per breath-hold. Precontrast T2w-HASTE images were acquired with TR = 4400 milliseconds, TE = 90 milliseconds, flip angle = 180°. A total of 30 slices were acquired in 2 breath-holds (15 slices per breath-hold) with an overall imaging time of 20 seconds per breath-hold. Pre- and postcontrast T1wGRE images were acquired with TR = 174.9 milliseconds, TE = 4.1 millisecond, flip angle = 80°. A total of 23 slices were acquired with an overall imaging time of 18–20 seconds depending on the field-of-view. The slice thickness for all sequences was 6 mm with an interslice gap of 1.5 mm. A matrix size of at least 160 × 256 was employed for all sequences with a rectangular field-of-view of 350–420 mm.

## Image Evaluation

Images were evaluated randomly in 2 sessions by 3 experienced off-site readers (L.G., G.M., S.S.; each with more than 10 years' experience in the field of liver MRI) who were fully blinded to all information regarding the clinical history of patients and the results of other diagnostic imaging examinations. Images were prepared on CD-ROM and sent by mail to each blinded reader for viewing and evaluation on each reader's personal computer. Image sets from each of the 60 patients were evaluated in each session. In the first session, each reader was presented with the unenhanced T2w and unenhanced T1wGRE images, the delayed T1wGRE images, and either the first or second set of dynamic T1wGRE images from each patient. In the second session, each reader was presented with the same unenhanced and delayed phase images but with the dynamic T1wGRE images not seen in the first session. The randomization of image sets for the first and second reading sessions was different and was determined by a central study coordinator (K.A.).

Each reader in each reading session was presented simultaneously with 6 image sets for each patient in a 3 × 2 arrangement on the computer screen. The upper row of images comprised, from left to right, the T2w image set, the unenhanced T1wGRE image set, and the enhanced T1wGRE hepatobiliary phase image set. The lower row displayed, from left to right according to the randomization scheme, the arterial, portal-venous, and equilibrium phase image sets from either the first or second dynamic series of acquisitions. Each of the 6 image sets on the screen contained images covering the entire liver, and the image levels were synchronized for the different techniques displayed. The readers were able to scroll through all image sets simultaneously or separately and were able to change the window setting, perform measurements and magnify the images.

The 3 blinded readers reported their findings for each patient on a case report form before moving to the image sets for the next patient. Only after the central study coordinator had received back from a reader the CD-ROM and completed case report forms for all 60 patients from the first reading session was the CD-ROM for the second reading session dispatched and the reader permitted to begin the second reading session. The interval between reading sessions was 28 days for reader 1, 21 days for reader 2, and 23 days for reader 3.

Each off-site blinded reader evaluated the image sets for all patients in an identical manner. Images were evaluated first for image quality and radiologic diagnosis (a 4-point scale where 1 = poor, 2 = sufficient, 3 = good, and 4 = excellent). Thereafter, each reader was asked whether any lesion was detected on the image sets and if so, how many. If 8 or fewer lesions were detected in a patient, the readers were asked to note the size and the liver segments in which they appeared (in terms of the segmental anatomy of the liver according to Couinaud[23] and Bismuth[24]) and to record their location on dedicated liver maps for subsequent matching between the first and second reading sessions. If more than 8 lesions were detected, the readers were asked to record the size and location of the 8 biggest lesions.

The enhancement patterns of lesions detected on both dynamic and delayed phase images were then recorded. For each lesion detected on dynamic phase images the readers were asked to characterize the enhancement pattern observed as indicative of a hypervascular lesion, a hypovascular lesion or a lesion demonstrating delayed persistent enhancement. For delayed phase images the readers were asked to decide whether the

detected lesions showed signal intensity enhancement or not. If enhancement was observed the readers were asked to decide whether this was homogenous or inhomogenous. If lesions were recorded as not showing enhancement, the readers were asked to decide whether these lesions had a hypointense rim surrounding the lesion or demonstrated signs of nonspecific peripheral wash-out. Frequently, delayed wash-in and wash-out of contrast may occur into central necrotic and fibrotic areas of hypovascular, nonenhancing lesions by a nonspecific mechanism, in a manner similar to that known from CT and from MRI with extracellular contrast agents. Finally, on the basis of the images evaluated, each reader was asked to make a diagnosis for each lesion detected.

## Accuracy for Lesion Characterization

The findings of the 3 blinded off-site readers were compared with the results of the on-site final diagnoses to evaluate the diagnostic efficacy for lesion characterization in the unenhanced liver versus lesion characterization in the pre-enhanced liver. For this assessment, the off-site findings for both sets of images were compared with histology results from either biopsy (36/60 patients, 60%; 55 lesions overall) or surgical resection (22/60 patients, 37%; 30 lesions overall). Lesion characterization for the remaining 2 patients was based on follow-up (1 patient with a large typical FNH) or autopsy (1 patient with alcohol-induced cirrhosis and more than 10 HCC lesions; autopsy performed within 1 month of the MR examination).

## Quantitative Evaluation

Quantitative evaluation of the enhancement behavior of lesions was performed by assessing the lesion signal intensity relative to normal liver on pre- and postcontrast T1-weighted images. Regions of interest (ROIs) matching the diameter of the lesion were placed on the lesion and the surrounding normal healthy liver parenchyma on images acquired precontrast and during each postcontrast phase of enhancement. ROIs in normal liver tissue were placed to the left or right of the lesion to avoid differences in SI caused by different distances to the body-array coil. An additional ROI was placed to determine the background noise. Care was taken to position each ROI in corresponding positions on each image set and on lesion and liver tissue whose signal intensities were as homogenous as possible. The relative lesion-to-liver contrast-to-noise ratio (CNR) for each lesion was determined according to the following equation:

$$CNR = \frac{SI_{Lesion} - SI_{Liver}}{SD_{noise}}$$

where $SI_{Lesion}$ = signal intensity measured at ROI positioned on the lesion, $SI_{Liver}$ = signal intensity measured at ROI positioned on the liver and $SD_{noise}$ = standard deviation of noise measured at ROI on nonenhancing extrahepatic tissue ventral to the upper abdomen.[25]

## Statistical Analysis

Cohen's kappa ($\kappa$) statistics were used to determine levels of agreement for lesion characterization for images

acquired in the unenhanced liver compared with images acquired in the pre-enhanced liver. Determinations were performed both for the differentiation of benign from malignant lesions and for the specific diagnosis of lesions relative to the final diagnosis for each patient. The percent agreement for lesion diagnosis against final diagnosis was also determined for images acquired in the unenhanced liver and pre-enhanced liver. Determinations of 3-reader agreement were performed for all images acquired after the first bolus injection of gadobenate dimeglumine in the unenhanced liver and for all images acquired after the second bolus injection in the pre-enhanced liver. Finally, evaluations were performed for malignant lesions and benign lesions separately.

## RESULTS

All image sets for all patients were considered to be of excellent diagnostic quality by each reader and all were included in the blinded assessments. All lesions detected during the first imaging session were visible also during the second imaging session. An on-site final diagnosis was available for all 60 patients. This was based on histology for 59 patients and patient follow-up for one patient.

## Malignant Lesions

Good overall agreement was obtained between the off-site blinded readers and the final on-site diagnosis for both the first and second sets of images. Malignant lesions that were detected but misdiagnosed as nonmalignant comprised a solitary metastasis from melanoma in a patient with 2 additional hemangiomas (misdiagnosed as hemangioma by reader 1 on pre-enhanced images only), a solitary metastasis from a leiomyosarcoma, which was misdiagnosed as hepatic adenoma by reader 3 on both image sets and by reader 2 on just the pre-enhanced image set, and a small (<1 cm) HCC, which tentatively was diagnosed as nonmalignant by readers 2 and 3 on both image sets. No other confirmed malignant lesion was misdiagnosed as nonmalignant by any reader on either of the 2 image sets.

Misdiagnoses among malignant lesions were made for one patient with 2 atypical nodules of HCC (misdiagnosed as metastases by all readers on both image sets), 1 patient with cholangiocellular carcinoma (misdiagnosed as metastasis by reader 1 on both image sets, and by reader 3 on the pre-enhanced image set only), and 1 patient with 2 nodules of fibrolamellar carcinoma (misdiagnosed as metastases or simply classified as "malignant" by all readers on both image sets). Imaging features considered characteristic of malignant lesions after contrast enhancement such as HCC pseudocapsule and early wash-out of contrast agent (Fig. 2) or peripheral hypervascularization or peripheral wash-out in metastases of colorectal carcinoma (Fig. 3) were clearly visualized both on conventional dynamic imaging after the first injection of gadobenate dimeglumine and on dynamic imaging in the pre-enhanced liver after the second injection of gadobenate dimeglumine.

## Benign Lesions

The 57 benign lesions determined on on-site final diagnosis in the 28 patients with 8 or fewer benign lesions
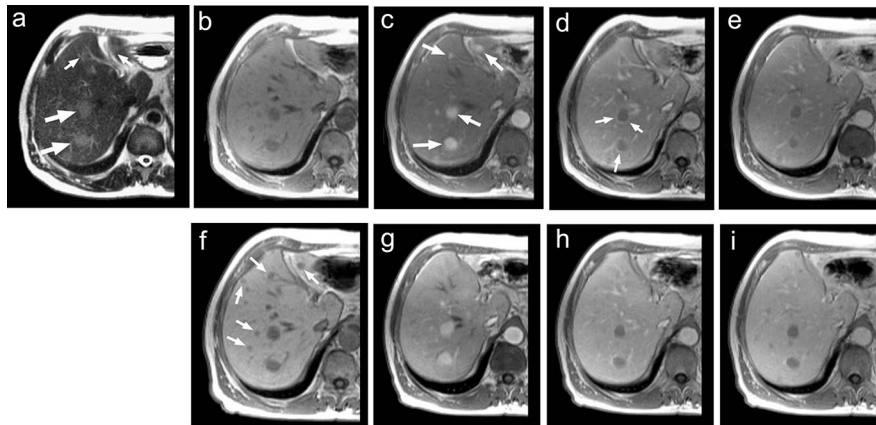
**FIGURE 2.** Multifocal HCC in a 58-year-old male patient. The unenhanced T2-weighted image (a) clearly reveals 2 focal areas (large arrows) of hyperintensity of approximately 2–3 cm diameter each in liver segments VII and VIII. Additional small areas of hyperintsity (small arrows) are also evident in segment IV and elsewhere. On the corresponding unenhanced T1-weighted image (b), these lesions are markedly hypointense against the surrounding normal parenchyma. During the arterial phase at 25 seconds after the first injection of gadobenate dimeglumine at 0.05 mmol/kg bodyweight (c), the lesions appear strongly hyperintense (arrows). However, the contrast has washed out completely by the portal-venous phase at 60 seconds (d), leaving the lesions as markedly hypointense with characteristic hyperintense peripheral rims (small arrows). This pattern of enhancement persists into the equilibrium phase at 5 minutes after injection (e). On the delayed phase image (f), the lesions are still strongly hypointense against the enhanced normal parenchyma although the peripheral rims can no longer be seen. Numerous small lesions (small arrows) identified as focal areas of hyperintensity during the arterial phase are clearly seen as hypointense during the delayed phase. A similar pattern of enhancement to that seen during the first dynamic series is seen during a second dynamic series (g, h, and i) acquired after a second injection of 0.05 mmol/kg gadobenate dimeglumine.
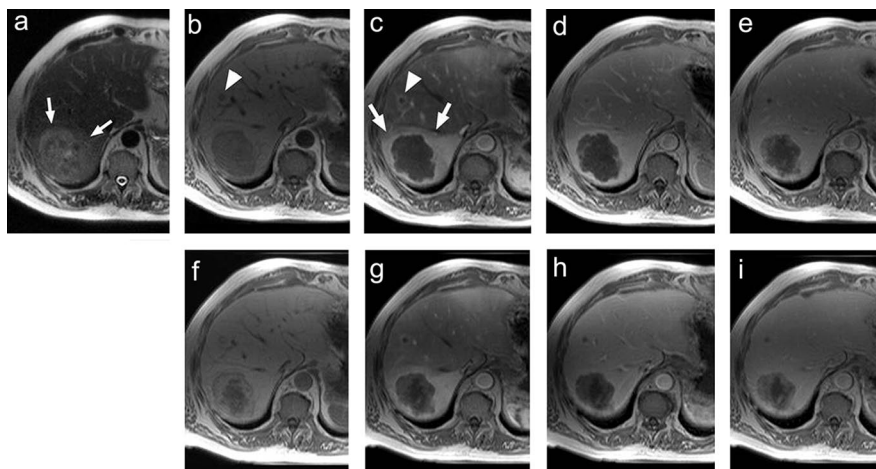


**FIGURE 3.** Metastases in a 64-year-old male patient with primary colorectal carcinoma. The unenhanced T2-weighted image (a) clearly reveals a large focal area (arrows) of hyperintensity of approximately 8 cm in liver segment VII. On the corresponding unenhanced T1-weighted image (b), this lesion is markedly hypointense against the surrounding normal parenchyma and a second, small hypointense area (arrowhead) is visible in liver segment VIII. During the arterial phase at 25 seconds after the first injection of gadobenate dimeglumine at 0.05 mmol/kg bodyweight (c), the large lesion is strongly hypointense and surrounded by a strongly hyperintense peripheral area (arrows). The second small lesion, not readily seen on the unenhanced T2-weighted image, can also be depicted together with a hyperintense rim (arrowhead), in liver segment VIII, indicating an infiltrative growth of the lesion. Both lesions are clearly seen as focal hypointense areas during the portal-venous (d) and equilibrium (e) phases after the first injection of gadobenate dimeglumine. On the delayed phase image (f) acquired at 60 minutes after injection both metastases have a characteristic target appearance. A similar pattern of behavior to that seen during the first dynamic series is seen during the second dynamic series (g, h, and i) acquired after a second injection of 0.05 mmol/kg gadobenate dimeglumine.

comprised 19 hemangiomas, 14 FNH, 8 adenomas, 8 cysts, 4 regenerative nodules, 1 subcapsular hematoma, 1 ecchinococal cyst, 1 regenerative hyperplasia, and 1 inflammatory pseudotumor. Complete agreement with the findings of the on-site final diagnosis was found for both image sets for the majority of patients with hemangioma. Among 11 patients

with just hemangioma, discrepancies in lesion diagnosis were noted for 3 patients by reader 1 (2 hemangiomas in 1 patient misdiagnosed as cysts on the first image set, 2 hemangiomas in 1 patient misdiagnosed as "unknown" on the first image set and as metastasis and cyst on the second image set, and 1 capillary hemangioma in 1 patient misdiagnosed as "unknown" on the second image set), for 1 patient by reader 2 (capillary hemangioma misdiagnosed as cholangiocellular carcinoma on the second image set) and for 3 patients by reader 3 (2 hemangiomas in 1 patient misdiagnosed as metastases on the second image set, 2 hemangiomas in another patient misdiagnosed as metastasis and cyst on the second image set, and the capillary hemangioma misdiagnosed as metastasis on the second image set).

Misdiagnoses among patients with just FNH were made by reader 1 only (1 atypical FNH in 1 patient misdiagnosed as metastasis on the first image set and another atypical FNH in another patient misdiagnosed as metastasis on the second image set). Examples of the enhancement of FNH and hemangioma after the first and second injections of gadobenate dimeglumine are shown in Figures 4 and 5. As in the case of malignant lesions, no differences between the first and second dynamic series were noted in terms of the visualization of typical features such as central scar in FNH.

Less good agreement between off-site readers and on-site final diagnoses was seen among patients with other types of benign lesion. A single hepatic adenoma in 1 patient (Fig. 6) was misdiagnosed by reader 1 as a metastasis on the first image set and as an HCC or FNH on the second image set. Similarly, a patient with 7 adenomas and a solitary FNH on on-site final diagnosis was misdiagnosed by reader 1 as

having 6 FNH or HCC on the first image set and 4 metastases or HCC on the second image set. The patients with regenerative nodules or regenerative hyperplasia were misdiagnosed by readers 2 and 3 on both image sets as having FNH or, in the case of a patient with a solitary regenerating nodule, as adenoma. In the case of reader 1, the solitary regenerating nodule was misdiagnosed as metastasis on the first image set and as HCC or FNH on the second image set whereas the lesions in the other patients were misdiagnosed as FNH or hemangioma. Each of the 3 readers misdiagnosed both the solitary inflammatory pseudotumor (reader 1 as HCC on both image sets and readers 2 and 3 as cholangiocellular carcinoma on both image sets) and the multiple abscesses (on all image sets as metastases). Finally, the subcapsular hematoma was misdiagnosed as adenoma on just the first image set by reader 1, as sarcoma and adenoma on the first and second image sets, respectively, by reader 2, and as HCC and adenoma on the first and second image sets, respectively, by reader 3.

## Reader (Interobserver) Agreement

High levels of agreement were obtained by each reader for comparisons of image sets acquired in the unenhanced liver and image sets acquired in the pre-enhanced liver. The overall agreement between image sets for the differentiation of benign from malignant lesions was $\kappa = 0.80$, $\kappa = 0.64$, and $\kappa = 0.56$ (readers 1, 2, and 3, respectively) whereas higher levels of agreement were obtained between image sets when evaluations were based on the specific diagnosis of lesions ($\kappa = 0.82$, $\kappa = 0.89$, and $\kappa = 0.86$; readers 1, 2, and 3, respectively). Separate comparisons of image sets for patients with malignant and benign lesions on final diagnosis
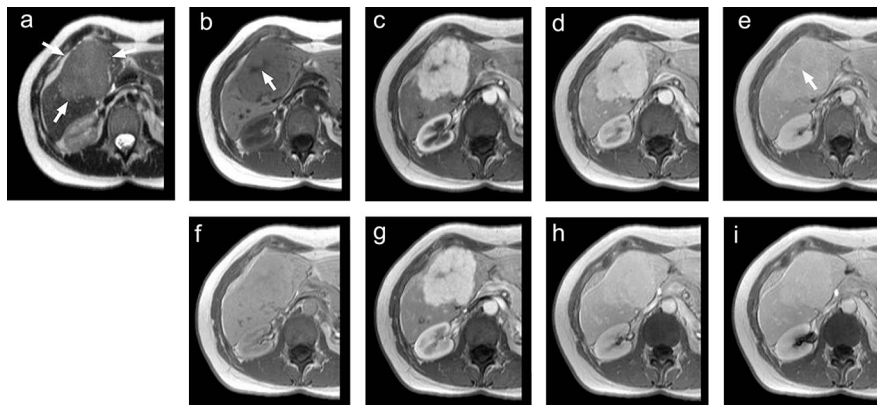


FIGURE 4. Typical FNH in a 34-year-old female patient. A large lesion (arrow) in liver segments IV and V is clearly seen as hyperintense against the surrounding liver parenchyma on the unenhanced T2-weighted image (a) and as hypointense on the unenhanced T1-weighted image (b). A hypointense central scar (arrow) within the lesion in (b) is suggestive of FNH. During the arterial phase at 25 seconds after the first injection of 0.05 mmol/kg gadobenate dimeglumine (c), the lesion appears as strongly hyperintense with a hypointense central scar. Contrast agent pooling during the portal-venous phase at 60 seconds (d) and the equilibrium phase at 5 minutes (e) after injection, combined with enhancement of the central scar (arrow in e) in the equilibrium phase, is highly suggestive of FNH. During the delayed phase (f) at 60 minutes after the injection of gadobenate dimeglumine, the lesion appears isointense to the surrounding parenchyma while the central scar is very faintly hypointense. A second dynamic series (g, h, and i) acquired after a second injection of 0.05 mmol/kg gadobenate dimeglumine reveals similar enhancement behavior to that seen during the first dynamic series although the more strongly enhanced surrounding normal parenchyma during the portal–venous phase (h) results in lower lesion-to-liver contrast and earlier uptake of contrast into the central scar.
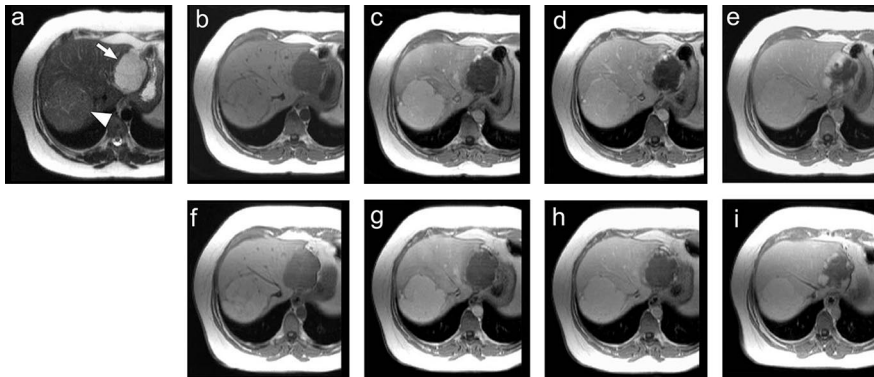
**FIGURE 5.** Atypical FNH and hemangioma in a 42-year-old female patient. The unenhanced T2-weighted image (a) reveals a large, strongly hyperintense lesion (arrow) in liver segment II and a faintly hyperintense lesion (arrowhead) in liver segments VII and VIII. The corresponding unenhanced T1-weighted image (b) reveals these lesions as markedly hypointense and isointense, respectively, against the surrounding normal parenchyma. During the dynamic series of acquisitions at 25 seconds (c), 60 seconds (d), and 5 minutes (e) after the first injection of 0.05 mmol/kg gadobenate dimeglumine, the lesion in segment II demonstrates an initial nodular peripheral enhancement followed by a centripetal "filling-in" pattern of contrast enhancement typical of hemangioma. Conversely, the lesion in segments VII and VIII shows rapid strong hyperintensity during the arterial phase (c) followed by contrast agent pooling during the portal-venous phase (d) and an isointense appearance during equilibrium (e) phase. Unlike the FNH in Figure 4, there is no evidence of a central scar in the lesion in segments VII and VIII. On the delayed phase image (f), the hemangioma is once again hypointense due to the wash-out of contrast agent while the FNH is faintly hyperintense to the surrounding normal parenchyma as the result of the specific uptake of gadobenate dimeglumine by the functioning hepatocytes present in FNH. Both lesions demonstrate similar enhancement patterns during a second dynamic series (g, h, and i) acquired after a second injection of 0.05 mmol/kg gadobenate dimeglumine.
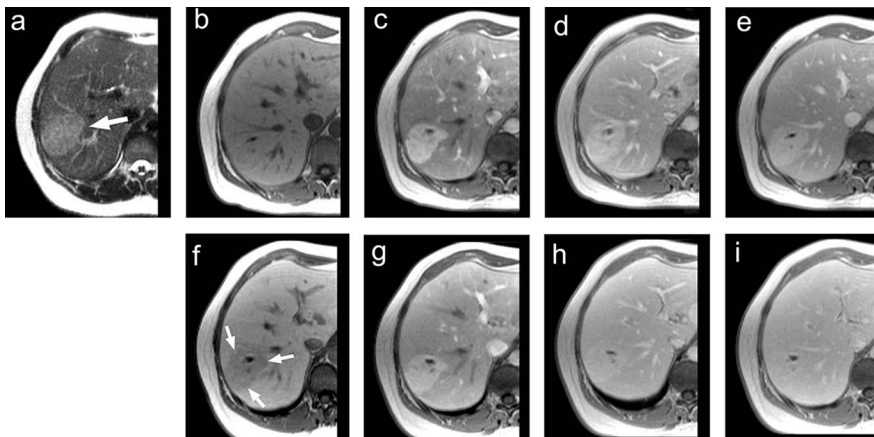


**FIGURE 6.** Hepatic adenoma in a 37-year-old female patient. A large lesion (arrow) is clearly seen in liver segment VII as slightly hyperintense against the surrounding liver parenchyma on the unenhanced T2-weighted image (a) and as isointense on the unenhanced T1-weighted image (b). During the arterial phase at 25 seconds after the first injection of 0.05 mmol/kg gadobenate dimeglumine (c), the lesion appears as strongly hyperintense. Thereafter, during the portal-venous phase at 60 seconds (d) and the equilibrium phase at 5 minutes (e) after injection the lesion demonstrates persistent hyperintensity due to contrast agent pooling in a manner similar to that observed with FNH. Unlike the enhancement behavior observed with FNH, the adenoma (arrows) is seen as hypointense against the enhanced normal parenchyma on the delayed phase image (f) acquired at 60 minutes postinjection. A similar pattern of enhancement to that seen during the first dynamic series is also seen during a second dynamic series (g, h, and i) acquired after a second injection of 0.05 mmol/kg gadobenate dimeglumine. However, the enhanced normal parenchyma at this time results in reduced lesion conspicuity, particularly on the portal-venous (h) and equilibrium (i) phase images.

revealed similarly high levels of agreement. For the 30 patients with malignant lesions, kappa values of $\kappa = 1.0$, $\kappa = 1.0$, and $\kappa = 0.89$ (readers 1, 2, and 3, respectively) were obtained for the comparison of images acquired in the unenhanced liver with images acquired in the pre-enhanced liver.

Agreement between image sets was similarly high for the 30 patients with benign lesions ($\kappa = 0.70$, $\kappa = 0.81$, and $\kappa = 0.83$; readers 1, 2, and 3, respectively).

Comparison between readers revealed similarly high levels of agreement. The agreement between the 3 readers for
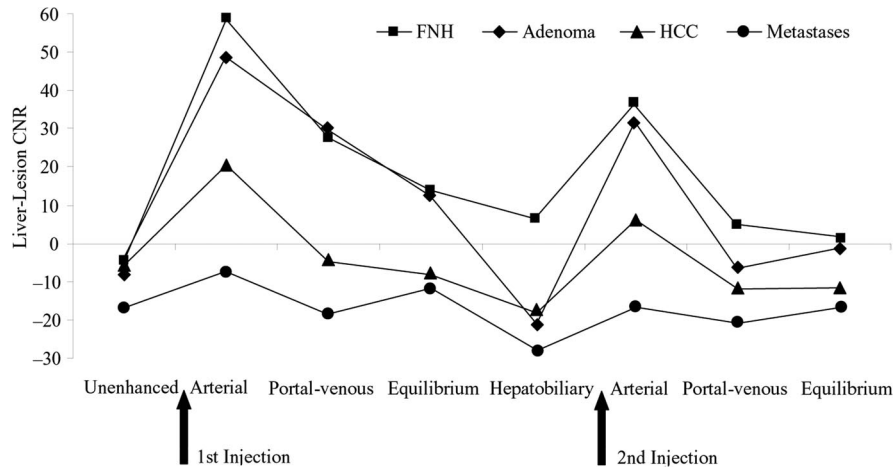
FIGURE 7. Mean liver-lesion CNRs on T1wGRE images during the dynamic and hepatobiliary phases after the first injection of 0.05 mmol/kg bodyweight gadobenate dimeglumine and during the dynamic phase after a second injection of 0.05 mmol/kg bodyweight gadobenate dimeglumine. The enhancement patterns are similar after both injections although the liver-lesion CNR after the second injection is reduced because of the enhanced normal liver parenchyma. Note that the magnitude of the CNR difference between hepatobiliary and unenhanced T1wGRE images is similar for FNH, adenoma, HCC and metastases although FNH appear hyperintense on hepatobiliary phase images relative to unenhanced images whereas adenoma, HCC and metastases appear hypointense reflecting the lack of Gd-BOPTA uptake into these lesions. A greater CNR difference between hepatobiliary and unenhanced T1wGRE images would have been obtained for all lesions had a dose of 0.1 mmol/kg bodyweight gadobenate dimeglumine been administered during the first injection (see ref.[18]).

the differentiation of benign from malignant lesions was $\kappa = 0.61$ for images acquired in the unenhanced liver (ie, using a standard imaging protocol) and $\kappa = 0.53$ for images acquired in the pre-enhanced liver (ie, using a time-efficient protocol). Corresponding agreement values for the specific diagnosis of lesions were $\kappa = 0.77$ and $\kappa = 0.72$, respectively. When patients with malignant and benign lesions were considered separately in terms of specific diagnosis, the 3-reader agreement for images acquired in the unenhanced liver was $\kappa = 0.66$ for malignant lesions and $\kappa = 0.83$ for benign lesions. For images acquired in the pre-enhanced liver the levels of agreement were $\kappa = 0.68$ for malignant lesions and $\kappa = 0.73$ for benign lesions.

The percent agreement for lesion diagnosis against on-site final diagnosis for each patient was high for each of the 3 blinded readers for both the image sets acquired in the unenhanced liver (75%, 81.7%, and 80% agreement; readers 1, 2, and 3, respectively) and for image sets acquired in the pre-enhanced liver (75%, 81.7%, and 75% agreement; readers 1, 2, and 3, respectively). Slightly better agreement with the on-site final diagnosis was noted for malignant lesions (83.3–86.7% for images acquired in the unenhanced liver; 80–86.7% for images acquired in the pre-enhanced liver) than for benign lesions (66.7–76.7% for images acquired in the unenhanced liver and for images acquired in the pre-enhanced liver).

## Quantitative Evaluation

The mean lesion-to-liver CNR values on T1-weighted images for the 4 most common histologically proven liver lesions (HCC, metastases, FNH, and adenoma) before and after each injection of 0.05 mmol/kg gadobenate dimeglumine are shown in Figure 7. The enhancement pattern of each lesion type on arterial phase images after the second injection of gadobenate dimeglumine was similar to that after the first

injection of gadobenate dimeglumine although the absolute mean CNR values for the hypervascular lesions were lower. Similarly reduced mean CNR values on portal–venous phase images after the second injection of gadobenate dimeglumine reflected the higher signal intensity of the enhanced normal liver parenchyma after the first injection of gadobenate dimeglumine.

Regarding the individual lesion types, the metastases in the present study were consistently hypointense to the normal liver parenchyma whereas the HCCs showed slight hyperintensity during the arterial phase after both injections of gadobenate dimeglumine. In contrast, the benign FNHs were consistently hyperintense to the normal liver parenchyma. The behavior of the adenomas resembled that of the FNHs after the first injection of gadobenate dimeglumine and during the arterial phase after the second injection of gadobenate dimeglumine. However, these lesions could be distinguished from FNH on the basis of their hypointense appearance on delayed phase images. Similar behavior for regenerating nodules and other lesion types was noted on images acquired after the second injection of gadobenate dimeglumine compared with images acquired after the first injection although in all cases the mean lesion-to-liver CNR values were lower.

## DISCUSSION

The incidence of liver metastases among patients with primary tumors elsewhere in the body is high: autopsy series of patients with extrahepatic primary tumors indicate that approximately 50% of patients have metastatic disease of the liver at the time of death.[26,27] Among the primary cancers considered most at risk for metastasizing to the liver are pancreatic, breast, lung, gastric, and colorectal cancer.[26,28]

**112**

Currently, MR examinations of the liver for the detection of liver metastases usually are conducted as independent procedures, distinct from the MR examination of the primary tumor. Unfortunately, the need to perform 2 or more MR examinations to accurately stage the extent of disease can impact greatly both on imaging time and costs. Although CT, particularly with multidetector systems, represents a cheaper, easier, and more rapid technique for cancer staging, this modality is limited by lower specificity and by the need for ionizing radiation and relatively large doses of iodinated contrast agent.[29–31] Furthermore, multidetector CT has not yet proven sufficiently specific for diagnosis of, for example, primary breast cancer.[32]

With contrast-enhanced MRI of the breast rapidly gaining acceptance for primary cancer screening, surgical planning and postsurgical follow-up,[33] and potential innovations in MRI of the lung for cancer detection,[34] the possibility to combine a contrast-enhanced MR examination of these organs with a dedicated enhanced screening examination of the liver may be of great interest. Unfortunately, the purely extracellular nature of most gadolinium contrast agents do not lend themselves to combined same-session imaging of both the extrahepatic tumor and liver. Moreover, there is some debate as to whether the detection of liver metastases is actually improved with the use of conventional gadolinium agents.[35] Purely liver-specific contrast agents are also inappropriate for a procedure of this type because of their unsuitability for MRI of extrahepatic tumors. Many of the drawbacks associated with the use of conventional gadolinium agents may be overcome with the use of gadobenate dimeglumine which combines the properties of a conventional extracellular agent with those of an agent targeted specifically to the liver.[13] Gadobenate dimeglumine is a safe gadolinium contrast agent[36,37] and is effective not only for all applications for which conventional agents are used[4–9,14–17,35,38–41] but also for delayed, static MRI of the liver.[11,12,14–22] As a consequence, the possibility to combine contrast-enhanced MRI of a primary extrahepatic tumor with a delayed screening examination for liver metastases may be feasible with this agent.

Unfortunately, the liver is not only a repository for metastatic disease. The worldwide incidence of primary malignant HCC has increased in recent years[42] whereas benign liver tumors not requiring surgical intervention have been observed in as many as 20% of the adult population.[43] A study by Schwartz et al[44] reported the presence of small hepatic lesions in 378 (12.7%) patients among 2978 patients with cancer and that of these lesions approximately 80% were presumed benign due to the lack of growth over a mean follow-up interval of 25.6 months. Because of the relatively high prevalence of benign lesions in the liver, it is clear that any screening or follow-up approach for metastases should also be able to adequately characterize lesions discovered incidentally during the MR imaging examination.

The present study proposes a novel, time-efficient MRI protocol for metastases screening that also permits same-session characterization of incidentally discovered liver lesions. Specifically, the present study confirms that the dynamic enhancement patterns of common benign and malignant liver lesions are similar and readily diagnostic regardless of whether images are acquired conventionally in an otherwise unenhanced liver, or after a second injection of gadobenate dimeglumine in a liver that is already enhanced from a first injection. Using the proposed protocol it may be possible to administer gadobenate dimeglumine at 1–3 hours ahead of the liver examination either directly to patients referred specifically for liver MRI or to patients with a primary extrahepatic tumor for whom an additional screening examination for liver metastases may be appropriate. The images acquired during this screening examination would thus be conventional T2w images and gadobenate dimeglumine-enhanced T1w images, both of which have been shown to improve the detection of metastases.[12,14,15,17,19] Thereafter, a second injection of gadobenate dimeglumine would be performed followed immediately by conventional dynamic phase imaging if a lesion is discovered incidentally for which additional characterization is required. However, it is important to note that a second injection would not always be necessary: there would be no need to administer a second dose and to perform a dynamic MR examination in patients with no unidentifiable lesions on T2w or hepatobiliary phase T1w images or in whom only hepatic metastases are present.

Likewise, the observation of imaging features considered typical of malignant lesions such as a peripheral hypointense rim on hepatobiliary phase T1w images or a doughnut appearance on T2w images may be sufficient to adequately characterize lesions as malignant without recourse to the additional information available on dynamic imaging. The option of a second injection would be appropriate only in patients with equivocal lesions on T2w and hepatobiliary phase T1w images (eg, small hyperenhancing hepatomas) for which the additional information available on dynamic imaging would facilitate accurate differential diagnosis. In this regard, small hyperenhancing lesions that are not seen on hepatobiliary phase T1w images are highly likely to be benign in nature.[22] On the other hand, certain well-differentiated HCC also may take up gadobenate dimeglumine and appear hyper- or isointense on delayed hepatobiliary phase imaging.[45] For these latter lesions, the appearance on T2w images might imply the need for further dynamic phase imaging or biopsy.

We emphasize that the 60 patients included in the present study were enrolled in a consecutive manner and were representative of a broad cross section of patients referred for MRI of the liver in daily routine practice. There was no preselection of patients with specific lesion types and no exclusion of patients on the basis of imaging findings. Furthermore, the 3 readers were fully blinded to all information regarding the clinical history of patients and the results of other diagnostic imaging examinations. Despite the wide variety of liver diseases included in the study and the tight control of information available to the readers, each reader demonstrated a high level of consistency between the 2 reading sessions in the ability to detect and diagnose focal liver lesions ($\kappa = 0.56-0.89$ for determinations of agreement for diagnoses made on the basis of images acquired in unenhanced liver and images acquired in pre-enhanced liver).

The principal finding of the study was that lesions that demonstrate characteristic enhancement behavior in the unenhanced liver after a first injection of gadobenate dimeglumine invariably demonstrate similar enhancement behavior in the pre-enhanced liver after a second injection of gadobenate dimeglumine. In support of this finding were the results of quantitative analyses, which revealed similar enhancement behavior after the second injection of gadobenate dimeglumine to the behavior observed after the first injection, particularly during the immediate postinjection arterial phase. The fact that the lesion-liver CNR was lower after the second injection can be ascribed to the higher background signal intensity of the enhanced normal liver parenchyma.

As regards the 3 confirmed malignant lesions (2 solitary metastases and an HCC) that were misdiagnosed at MRI, the misdiagnosis of the small HCC may be attributed to the absence of characteristic morphologic features which are typically seen only in larger HCCs and to the fact that HCCs demonstrate variable enhancement patterns on T1w images, ranging from markedly hypointense to markedly hyperintense.[45–47] In the case of the 2 misdiagnosed metastases, these were from patients with primary melanoma and primary leiomyosarcoma: primary tumors whose metastases are known to be hypervascular and to demonstrate hyperintensity compared with the normal parenchyma on arterial phase images.[48]

Of particular interest was the enhancement behavior of benign FNH and hepatic adenoma. These lesions often are difficult to differentiate on enhanced MRI with conventional gadolinium chelates but are readily differentiated on delayed MRI after gadobenate dimeglumine.[22] The differential enhancement behavior of these lesions clearly was demonstrated both qualitatively and quantitatively in the present study. Interestingly, off-site reader 1 who had only limited experience of gadobenate dimeglumine was unaware of this differential diagnostic feature and misdiagnosed all of the adenomas in the study. Conversely, off-site readers 2 and 3 who use gadobenate dimeglumine routinely for liver MRI successfully diagnosed all of the adenomas on both image sets.

To note is that gadobenate dimeglumine at a dose of 0.05 mmol/kg bodyweight was used for both injections in the study. Although gadobenate dimeglumine at this dose has previously been shown to be equivalent to gadopentetate dimeglumine at a dose of 0.1 mmol/kg bodyweight because of the higher relaxivity of gadobenate dimeglumine in vivo,[11] for liver screening studies conducted in conjunction with MR imaging of the primary tumor, it is likely that a higher dose of 0.1 mmol/kg bodyweight would be the initial dose administered. In early studies a dose of 0.1 mmol/kg gadobenate dimeglumine was shown to produce significantly greater enhancement of normal liver parenchyma on delayed images compared with a dose of 0.05 mmol/kg gadobenate dimeglumine.[12,18] It is unclear whether a first dose of 0.1 mmol/kg used for MRI of the primary tumor would subsequently influence the dynamic enhancement behavior of liver lesions after a second injection of 0.05 mmol/kg gadobenate dimeglumine. Although it is possible a lower lesion–liver CNR

would be attained for hypervascular lesions during the arterial phase after the second injection, it is equally possible the greater enhancement of normal liver parenchyma before the second injection would improve the effectiveness of the original screening for metastases.

Currently, a standard liver imaging protocol for gadobenate dimeglumine would involve T1w acquisitions during the dynamic phase of contrast enhancement followed, if additional diagnostic information is required, by acquisitions during the delayed hepatobiliary phase between 1 and 3 hours after administration.[11,14–17] However, although such a protocol can maximize the amount of diagnostic information acquired, the need to remove patients from the magnet after the initial series of dynamic acquisitions and then reinsert them at 1–3 hours after injection for acquisition of delayed images may be considered a drawback, particularly in busy institutions with a high daily throughput of patients. The advantage of the proposed protocol is in the improved time-efficiency and patient-friendliness of the procedure: patients are required to enter the magnet only once and acquisition of dynamic and delayed phase information is obtained in little more than the time required to obtain solely dynamic phase information with conventional gadolinium agents.

Although the present study clearly shows that similar diagnostic information can be acquired using the modified imaging protocol, the findings require further substantiation particularly in patients at risk for metastatic liver disease in whom the benefits of gadobenate dimeglumine for both detection of metastases and characterization of incidental lesions are likely to be most appreciated.

## REFERENCES

1. Pintaske J, Martirosian P, Graf H, et al. Relaxivity of gadopentetate dimeglumine (Magnevist), gadobutrol (Gadovist), and gadobenate dimeglumine (MultiHance) in human blood plasma at 0.2, 1.5, and 3 Tesla. *Invest Radiol.* 2006;41:213–221. Erratum in *Invest Radiol.* 2006;41:859.
2. Cavagna FM, Maggioni F, Castelli PM, et al. Gadolinium chelates with weak binding to serum proteins: a new class of high-efficiency, general purpose contrast agents for magnetic resonance imaging. *Invest Radiol.* 1997;32:780–796.
3. Giesel FL, von Tengg-Kobligk H, Wilkinson ID, et al. Influence of human serum albumin on longitudinal and transverse relaxation rates (r1 and r2) of magnetic resonance contrast agents. *Invest Radiol.* 2006;41:222–228.
4. Knopp MV, Runge VM, Essig M, et al. Primary and secondary brain tumors at MR imaging: bicentric intraindividual crossover comparison of gadobenate dimeglumine and gadopentetate dimeglumine. *Radiology.* 2004;230:55–64.
5. Knopp MV, Giesel FL, von Tengg-Kobligk H, et al. Contrast-enhanced MR angiography of the run-off vasculature: intraindividual comparison of gadobenate dimeglumine with gadopentetate dimeglumine. *J Magn Reson Imaging.* 2003;17:694–702.
6. Prokop M, Schneider G, Vanzulli A, et al. Contrast-enhanced MR angiography of the renal arteries: blinded multicenter crossover comparison of gadobenate dimeglumine and gadopentetate dimeglumine. *Radiology.* 2005;234:399–408.
7. Pediconi F, Catalano C, Occhiato R, et al. Breast lesion detection and characterization at contrast-enhanced MR mammography: gadobenate dimeglumine versus gadopentetate dimeglumine. *Radiology.* 2005;237:45–56.
8. Essig M, Lodemann KP, Le-Huu M, et al. Intraindividual comparison of gadobenate dimeglumine and gadobutrol for cerebral magnetic resonance perfusion imaging at 1.5 T. *Invest Radiol.* 2006;41:256–263.
9. Runge VM, Biswas J, Wintersperger BJ, et al. The efficacy of gado-

benate dimeglumine (Gd-BOPTA) at 3 Tesla in brain magnetic resonance imaging: comparison to 1.5 Tesla and a standard gadolinium chelate using a rat brain tumor model. *Invest Radiol.* 2006;41:244–248.

10. Wersebe A, Wiskirchen J, Decker U, et al. Comparison of Gadolinium-BOPTA and Ferucarbotran-enhanced three-dimensional T1-weighted dynamic liver magnetic resonance imaging in the same patient. *Invest Radiol.* 2006;41:264–271.

11. Schneider G, Maas R, Schultze Kool L, et al. Low-dose gadobenate dimeglumine versus standard dose gadopentetate dimeglumine for contrast-enhanced magnetic resonance imaging of the liver: an intra-individual crossover comparison. *Invest Radiol.* 2003;38:85–94.

12. Spinazzi A, Lorusso V, Pirovano G, et al. Safety, tolerance, biodistribution and MR imaging enhancement of the liver with gadobenate dimeglumine: results of clinical pharmacologic and pilot imaging studies in nonpatient and patient volunteers. *Acad Radiol.* 1999;6:282–291.

13. Kirchin MA, Pirovano G, Spinazzi A. Gadobenate dimeglumine (gadobenate dimeglumine): an overview. *Invest Radiol.* 1998;33:798–809.

14. Pirovano G, Vanzulli A, Marti-Bonmati L, et al. Evaluation of the accuracy of gadobenate dimeglumine-enhanced MR imaging in the detection and characterization of focal liver lesions. *AJR Am J Roengenol.* 2000;175:1111–1120.

15. Kim YK, Lee JM, Kim CS. Gadobenate dimeglumine-enhanced liver MR imaging: value of dynamic and delayed imaging for the characterization and detection of focal liver lesions. *Eur Radiol.* 2004;14:5–13.

16. Kim YK, Kim CS, Lee YH, et al. Comparison of superparamagnetic iron oxide-enhanced and gadobenate dimeglumine-enhanced dynamic MRI for detection of small hepatocellular carcinomas. *AJR Am J Roentgenol.* 2004;182:1217–1223.

17. Kim YK, Lee JM, Kim CS, et al. Detection of liver metastases: gadobenate dimeglumine-enhanced three-dimensional dynamic phases and one-hour delayed phase MR imaging versus superparamagnetic iron oxide-enhanced MR imaging. *Eur Radiol.* 2005;15:220–228.

18. Spinazzi A, Lorusso V, Pirovano G, et al. MultiHance clinical pharmacology: biodistribution and MR enhancement of the liver. *Acad Radiol.* 1998;5:S86–S89.

19. Caudana R, Morana G, Pirovano G, et al. Focal malignant hepatic lesions: MR imaging enhanced with gadolinium benzyloxypropionictetra-acetate (BOPTA)—preliminary results of phase II clinical application. *Radiology.* 1996;199:513–520.

20. Petersein J, Spinazzi A, Giovagnoni A, et al. Focal liver lesions: evaluation of the efficacy of gadobenate dimeglumine in MR imaging—a multicenter phase III clinical study. *Radiology.* 2000;215:727–736.

21. Grazioli L, Morana G, Federle MP, et al. Focal nodular hyperplasia: morphological and functional information from MR imaging with gadobenate dimeglumine. *Radiology.* 2001;221:731–739.

22. Grazioli L, Morana G, Kirchin MA, et al. Accurate differentiation of focal nodular hyperplasia from hepatic adenoma at gadobenate dimeglumine-enhanced MR imaging: prospective study. *Radiology.* 2005; 236:166–177.

23. Couinaud C. *Le foie: études anatomiques et chirurgicales.* Paris: Masson; 1957:9–12.

24. Bismuth H. Surgical anatomy and anatomical surgery of the liver. *World J Surg.* 1982;6:3–8.

25. Schima W, Petersein J, Hahn PF, et al. Contrast-enhanced MR imaging of the liver: comparison between Gd-BOPTA and Mangafodipir. *J Magn Reson Imaging.* 1997;7:130–135.

26. Baker ME, Pelley R. Hepatic metastases: basic principles and implications for radiologists. *Radiology.* 1995;197:329–337.

27. Abrams HL, Spiro R, Goldstein N. Metastases in carcinoma; analysis of 1000 autopsied cases. *Cancer.* 1950;3:74–85.

28. Lewis KH, Chezmar JL. Hepatic metastases. *Magn Reson Imaging Clin N Am.* 1997;5:319–330.

29. Semelka RC, Cance WG, Marcos HB, et al. Liver metastases: comparison of current MR techniques and spiral CT during arterial portography for detection in 20 surgically staged cases. *Radiology.* 1999;213:86–91.

30. Semelka RC, Martin DR, Balci C, et al. Focal liver lesions: comparison of dual-phase CT and multisequence multiplanar MR imaging including dynamic gadolinium enhancement. *J Magn Reson Imaging.* 2001;13:397–401.

31. Sica GT, Ji H, Ros PR. Computed tomography and magnetic resonance imaging of hepatic metastases. *Clin Liver Dis.* 2002;6:165–179.

32. Inoue M, Sano T, Watai R, et al. Dynamic multidetector CT of breast tumors: diagnostic features and comparison with conventional techniques. *AJR Am J Roentgenol.* 2003;181:679–686.

33. Thibault F, Nos C, Meunier M, et al. MRI for surgical planning in patients with breast cancer who undergo preoperative chemotherapy. *AJR Am J Roentgenol.* 2004;183:1159–1168.

34. Schroeder T, Ruehm SG, Debatin JF, et al. Detection of pulmonary nodules using a 2D HASTE MR sequence: comparison with MDCT. *AJR Am J Roentgenol.* 2005;185:979–984.

35. Hamm B, Mahfouz AE, Taupitz M, et al. Liver metastases: improved detection with dynamic gadolinium-enhanced MR imaging? *Radiology.* 1997;202:677–682.

36. Kirchin MA, Pirovano G, Venetianer C, et al. Safety assessment of gadobenate dimeglumine (Multihance®): extended clinical experience from phase I studies to post-marketing surveillance. *J Magn Reson Imaging.* 2001;14:281–294.

37. Shellock FG, Parker JR, Venetianer C, et al. Safety of gadobenate dimeglumine (MultiHance): summary of findings from clinical studies and postmarketing surveillance. *Invest Radiol.* 2006;41:500–509.

38. Schneider G, Kirchin MA, Pirovano G, et al. Gadobenate dimeglumine-enhanced magnetic resonance imaging of intracranial metastases: effect of dose on lesion detection and delineation. *J Magn Reson Imaging.* 2001;14:525–539.

39. Knopp MV, Bourne MW, Sardanelli F, et al. Gadobenate dimeglumine-enhanced MRI of the breast: analysis of dose response and comparison with gadopentetate dimeglumine. *Am J Roengenol.* 2003;181:663–676.

40. Völk M, Strotzer M, Lenhart M, et al. Renal time-resolved MR angiography: quantitative comparison of gadobenate dimeglumine and gadopentetate dimeglumine with different doses. *Radiology.* 2001;220:484–488.

41. Anzalone N, Scomazzoni F, Castellano R, et al. Carotid artery stenosis: intra individual correlations of 3D time-of-flight MR angiography, contrast-enhanced MR angiography, conventional DSA, and rotational angiography for detection and grading. *Radiology.* 2005;236:204–213.

42. Llovet JM, Burroughs A, Bruix J. Hepatocellular carcinoma. *Lancet.* 2003;362:1907–1917.

43. Karhunen PJ. Benign hepatic tumors and tumor-like conditions in man. *J Clin Pathol.* 1986;39:183–188.

44. Schwartz LH, Gandras EJ, Colangelo SM, et al. Prevalence and importance of small hepatic lesions found at CT in patients with cancer. *Radiology.* 1999;210:71–74.

45. Grazioli L, Morana G, Caudana R, et al. Hepatocellular carcinoma: correlation between gadobenate dimeglumine-enhanced MRI and pathologic findings. *Invest Radiol.* 2000;35:25–34.

46. Yamashita Y, Fan ZM, Yamamoto H, et al. Spin-echo and dynamic gadolinium-enhanced FLASH MR imaging of hepatocellular carcinoma: correlation with histopathologic findings. *J Magn Reson Imaging.* 1994; 4:83–90.

47. Hussain SM, Semelka RC, Mitchell DG. MR imaging of hepatocellular carcinoma. *Magn Reson Imaging Clin N Am.* 2002;10:31–52.

48. Kelekis NL, Semelka RC, Woosley JT. Malignant lesions of the liver with high signal intensity on T1-weighted MR images. *J Magn Reson Imaging.* 1996;6:291–294.